JOURNAL OF Materials CHEMISTRY

Organic/inorganic molecular conductors based upon perylene and Lindquist-type polyoxometalates†

Miguel Clemente-León,[a] Eugenio Coronado,*[a] Carlos Giménez-Saiz,[a] Carlos J. Gómez-García,[a] Eugenia Martínez-Ferrero,[a] Manuel Almeida[b] and Elsa B. Lopes[b]

[a]*Instituto de Ciencia Molecular, Universidad de Valencia, E-46100 Burjassot, Spain. E-mail: eugenio.coronado@uv.es*
[b]*Instituto Tecnológico e Nuclear, P-2686 Sacavém, Portugal*

Received 4th April 2001, Accepted 23rd May 2001
First published as an Advance Article on the web 13th July 2001

The preparation, structures and physical properties of the organic/inorganic radical salts based upon perylene (per) and Lindquist type polyoxometalates (POMs) are reported. Three new hybrid salts have been prepared: $(per)_5[Mo_6O_{19}]$ (**1**), $(per)_5[W_6O_{19}]$ (**2**), and $(per)_5[VW_5O_{19}]$ (**3**). Only structures **1** ($P\bar{1}$, $Z=2$) and **3** ($P\bar{1}$, $Z=2$) were fully determined as compound **2** was found to have unit cell parameters practically identical to **1** and, therefore, is considered isostructural with the latter. The structures consist of interpenetrated organic and mixed organic/inorganic layers in the *ac* plane alternating along the *a* direction. The organic layers present a novel packing mode of the perylene molecules that consists of criss-cross chains formed by two alternating dimers running along the *c* axis. Besides the ability to induce novel packings in the organic sublattice, the possibility offered by the POMs of varying the charge while maintaining the size and shape of the anion has enabled the control of the electronic band filling and, therefore, of the electrical and magnetic properties. Thus, salts **1** and **2**, where the anionic charge is −2, are diamagnetic and present lower room temperature conductivities, while salt **3**, where the anionic charge is −3, has an unpaired electron and presents a higher room temperature conductivity and a lower activation energy. Thermopower measurements show that salts **1** and **2** present hole-type conduction whereas salt **3** exhibits electron-dominating electrical transport.

Introduction

The preparation of compounds formed by two molecular networks is receiving great attention nowadays as they provide a source of novel materials with unusual physical properties or combinations of properties. Significant efforts have been devoted to organic/inorganic solids formed by stacks of partially oxidised π-electron organic donor molecules, which support electronic conduction, with charge-compensating transition metal complexes. These inorganic anions can act as structural or magnetic components leading to novel packing modes in the organic network, or to hybrid materials combining electrical with magnetic properties. Some relevant examples worth mentioning are the paramagnetic conductors[1] and superconductors[2] obtained by combining the discrete paramagnetic anions $[M(ox)_3]^{3-}$ ($M=Fe^{III}$ and Cr^{III}; ox = oxalate) and $[MX_4]^-$ ($M=Fe^{III}$, $X=Cl^-$, Br^-) with the organic donor bis(ethylenedithio)tetrathiafulvalene (BEDT-TTF) or its selenium derivative bis(ethylenedithio)tetraselenafulvalene (BETS), and the ferromagnetic conductor formed by the polymeric magnetic anion $[Mn^{II}Cr^{III}(ox)_3]^-$ and BEDT-TTF.[3]

In view of their unique molecular characteristics, polyoxometalate (POM) complexes have also been extensively used to obtain these types of functional molecular solids.[4] Owing to their specific shapes and large sizes and charges, these molecular metal-oxides have been shown to stabilise many unprecedented structural packing modes in the organic component. In most of them the electrons are strongly localised and show semiconducting behaviour, but in a few cases large electronic conductivities and metallic behaviour are also observed.[5] On the other hand, since they are electron acceptors and can incorporate one or more paramagnetic centres at specific sites of the polyoxoanion structure, they have enabled the formation of materials with the coexistence of delocalised electrons in both sublattices,[6] or with the coexistence of localised magnetic moments and delocalised electrons.[7] So far however only the TTF-type donors have been used to construct these hybrid molecular materials.

As part of our work in this area, we explore here the combination of POMs with the perylene molecule (Fig. 1a) which is one of the most frequently used donors in the preparation of highly conducting organic solids.[8] In fact, perylene has been used to produce many cation-radical salts with simple inorganic monoanions (Br^-,[9] I^-,[10] ClO_4^-,[11] or PF_6^- and AsF_6^-[12]) and charge-transfer salts with organic acceptors such as TCNQ[13] and perfluoroanil.[14] Electrical conductivities at room temperature up to 1400 S cm^{-1} have been measured in some cases. On the other hand, perylene salts with magnetic anions such as FeX_4^- ($X^-=Cl$, Br)[15] and

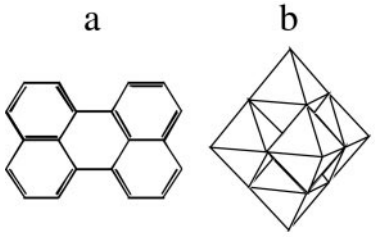

Fig. 1 (a) The perylene molecule. (b) Structure of the Lindquist polyanion.

†Electronic supplementary information (ESI) available: labelling schemes, complete crystallographic tables, atomic coordinates, thermal parameters, bond distances and angles of the asymmetric units of **1** and **3**. See http://www.rsc.org/suppdata/jm/b1/b103032a/

 DOI: 10.1039/b103032a

$M(mnt)^-$ anions (M = Au, Co, Cu, Fe, Ni, Pd, Pt; mnt = maleonitriledithiolate)[16] have also been reported. The latter series constitutes a unique example of the coexistence of conducting organic chains with magnetic inorganic chains.

A general feature of perylene salts is their one-dimensional electronic character due to the absence of atoms on the perylene molecule that can allow in-plane interactions. Thus, the transport properties of perylene-containing solids are mostly determined by the packing pattern of the organic molecules and their degree of partial oxidation. While the former depends on the geometry and volume of the anion, the charge distribution within the organic stacks varies with the number of charge-compensating anions and the charge thereon. In this context, we report here the synthesis, structure and physical properties of the radical cation salts based on perylene with three POMs of the Lindquist type, namely $[Mo_6O_{19}]^{2-}$, $[W_6O_{19}]^{2-}$, and $[VW_5O_{19}]^{3-}$ (Fig. 1b). As these polyanions have the same size and shape but two different charges, they offer the opportunity to study the differences induced by the variation of this charge on the transport and magnetic properties of the perylene salts.

Results and discussion

Crystal structures

From the unit cell parameters determined on single crystals of the three salts (see Table 1), we can conclude that salts **1** and **2** are isostructural whereas the unit cell angles and *b* parameter for salt **3** are slightly different to those of salts **1** and **2**. Therefore, we have fully determined the structure of salts **1** and **3**. Although there are small differences in some distances, the overall structures of salts **1** and **3** are very similar.

In both structures we can distinguish in the *ac* plane a mixed per/POM layer, where isolated perylene molecules (C-type) alternate with POM clusters (both located at inversion centres) and an organic layer formed by perylene molecules stacked in almost regular chains (Fig. 2). The organic layer is made up of perylene chains running along the *c* direction (Fig. 2). These chains are formed by two types of parallel crystallographically independent perylene molecules (A and B, located in general positions) packed in the sequence …AABB… There are one C-type, two A-type and two B-type perylene molecules per anion, giving the overall stoichiometry of 5 : 1.

The dimerised sequence and the fact that the long axis of the A molecule is tilted by 42° in **1** (40° in **3**) with respect to the

Table 1 Unit cell parameters for the salts $(per)_5[Mo_6O_{19}]$ (**1**), $(per)_5[W_6O_{19}]$ (**2**) and $(per)_5[VW_5O_{19}]$ (**3**) (per = perylene) and crystallographic parameters for salts **1** and **3**

	1	**2**	**3**
Formula	$C_{100}H_{60}Mo_6O_{19}$	$C_{100}H_{60}W_6O_{19}$	$C_{100}H_{60}VW_5O_{19}$
fw	2141.22	2668.68	2535.77
Crystal system	Triclinic	Triclinic	Triclinic
a/Å	10.983(5)	10.977(3)	10.9272(9)
b/Å	12.899(2)	12.951(2)	12.7077(11)
c/Å	13.627(7)	13.612(3)	13.5723(12)
α/°	83.21(2)	82.83(2)	82.139(2)
β/°	81.05(4)	81.00(2)	83.347(2)
γ/°	82.20(2)	82.17(2)	81.423(2)
V/Å^3	1880.0(13)	1882.6(8)	1837.3(3)
Space group	$P\bar{1}$	$P\bar{1}$	$P\bar{1}$
Z	2	2	2
$\mu(MoK_\alpha)$/mm^{-1}	1.053		8.001
Reflections indep.	6595		10746
R_{int}	0.0250		0.0553
R^a	0.0350		0.0562
R_ω	0.0779[b]		0.1272[c]

[a] $R = \Sigma(F_o - F_c)/\Sigma(F_o)$. [b] $R_\omega = [\Sigma[\omega(F_o^2 - F_c^2)^2]/\Sigma[\omega(F_o^2)^2]]^{1/2}$; $\omega = 1/[\sigma^2(F_o^2) + (0.0456P)^2]$, where $P = (F_o^2 + 2F_c^2)/3$. [c] $R_\omega = [\Sigma[\omega(F_o^2 - F_c^2)^2]/\Sigma[\omega(F_o^2)^2]]^{1/2}$; $\omega = 1/[\sigma^2(F_o^2) + (0.0786P)^2]$, where $P = (F_o^2 + 2F_c^2)/3$.

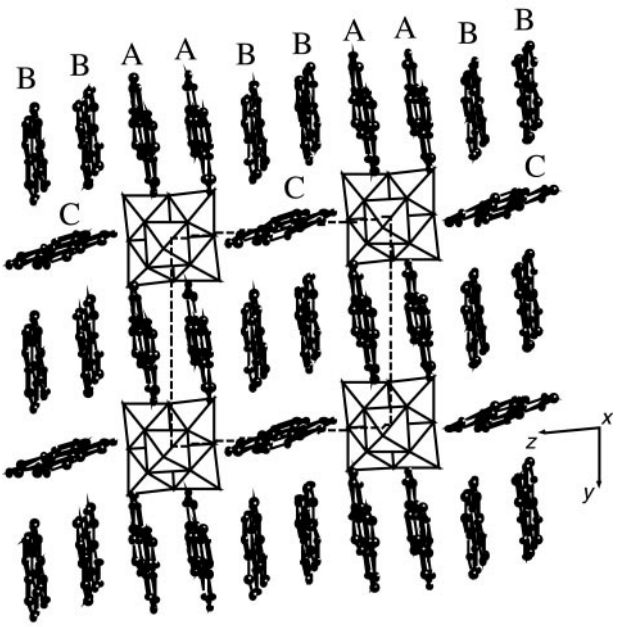

Fig. 2 View of the alternating layers in the *bc* plane of **1** showing the perylene molecules.

Fig. 3 View of the structure of the perylene chains along the *c* axis in **1** showing the overlapping mode of the A- (in black) and B-type (in white) perylene molecules. C-type perylene molecules are perpendicular to the axis chains (in grey).

B molecule (Fig. 3), suggest that the chains can be viewed as a criss-cross type arrangement formed by two alternating dimers. Nevertheless, as the intra- and interdimer distances are quite similar in the two solved structures and the packed molecules are almost parallel, the chains can be better described as a continuous stack of extensively overlapping parallel molecules (carrying partial charges) with almost uniform interplanar separations. Thus, the intradimer distances are very similar in the AA (3.39 Å in **1** and 3.32 Å in **3**) and in the BB (3.48 Å in **1** and 3.41 Å in **3**) dimers and are also very close to the interdimer distances (3.35 Å in **1** and 3.38 Å in **3**). Moreover, A and B molecules are almost parallel with slip angles less than 2° in both structures. As observed in other structures, the perylene molecules are not perfectly eclipsed but slightly shifted to minimise the intermolecular distances. In both structures the shifts along the long (Δx) and short (Δy) molecular axes are bigger in the BB dimers ($\Delta x = 0.80/0.10$ Å; $\Delta y = 0.85/0.90$ Å in **1** and **3**, respectively) than in the AA ones ($\Delta x = 0.15/0.05$ Å; $\Delta y = 0.30/0.50$ Å in **1** and **3**, respectively). Nevertheless, they are small compared with the molecular size. This regular arrangement favours the electron delocalization and accounts for the high room temperature conductivities found in the three salts (see below). It is important to note that the intra- and interdimer distances are very similar in both **1** and **3** suggesting that the size and the shape of the anion are the factors determining the packing in the three salts, even if the anionic charge is different (−2 in salts **1** and **2** and −3 in salt **3**).

The only appreciable, but very important, effect of the anionic charge deals with the charge distribution in the organic molecules. Thus, assuming that perylene molecule C remains neutral, based on the instability showed by isolated perylene radicals, especially in dichloromethane solvent,[17] the stacked perylene molecules A and B have an average oxidation state of $(per)_4^{2+}$ in compounds **1** and **2**, while in compound **3** their average oxidation state is $(per)_4^{3+}$. If the stacks were regular these degrees of partial oxidation would lead to single band systems filled up to 3/4 and 5/8 respectively, with metallic properties in all cases (Fig. 4a). However, in the three salts there are four stacked perylene molecules per unit cell, and this tetramerization of the chains leads to a fourfold splitting of the original band originating from the HOMO, with the opening of three gaps as shown schematically in Fig. 4. These three gaps are expected to be present in the three salts (as they all show the same type of crystal packing) with small variations due to the slight changes in the intermolecular distances that will produce small differences in the electronic intermolecular interactions.

The presence of these three gaps imposes dramatic differences in the physical properties of the systems depending on their band filling. Compounds **1** and **2** are predicted to be semiconductors with the Fermi level at the middle of the upper gap (Fig. 4b). Compound **3** is predicted to present a half-filled band which was full in compounds **1** and **2**. However, this relatively narrow and half-filled band, due to sizeable electronic correlation interactions, is expected to lead to a Mott insulator rather than to a metal as depicted in Fig. 4c. The effects of the different band fillings are indeed seen in the physical properties.

Focusing on the mixed organic/inorganic layer, both structures are almost identical. The only difference involves the size of the anion, which is slightly bigger in salt **1** (where the average Mo···Mo distance in the $[Mo_6O_{19}]^{2-}$ anion is 4.64 Å) than in salt **3** (where the average W···W distance in the $[VW_5O_{19}]^{3-}$ anion is 4.61 Å). In this anion the V site is delocalised over the six metallic sites of which three are independent.

Physical properties

The magnetic properties of the three compounds are plotted in Fig. 5. For compounds **1** and **2** the magnetic susceptibility data indicate a complete pairing of the electrons in the perylene chains, even at room temperature, compatible with the full band semiconductor picture of Fig. 4b. Thus, both salts are weakly paramagnetic showing very low Curie constant values of 0.07 and 0.04 emu K mol^{-1} (Fig. 5a), which may be attributed to small amounts of paramagnetic impurities ($\sim$0.2 and 0.1 unpaired electrons per formula unit, respectively). For salt **3**, the value of the Curie constant is 0.4 emu K mol^{-1}, and it decreases as the temperature is lowered. This result indicates the presence of one unpaired electron per formula unit; the spins of these electrons are

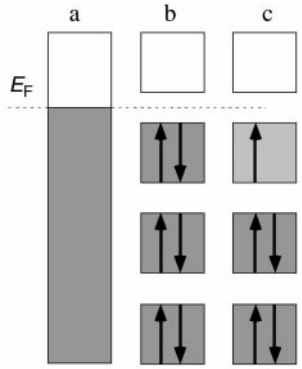

Fig. 4 Schematic band filling diagram for a uniform $(per)_4^{2+}$ stack (a), a tetramerized $(per)_4^{2+}$ stack (b) and a tetramerized $(per)_4^{3+}$ stack (c).

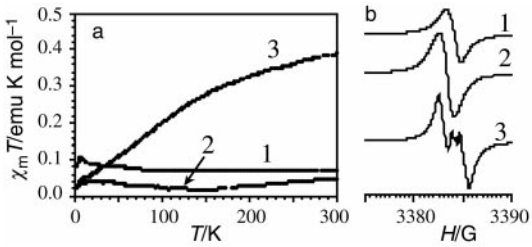

Fig. 5 (a) Thermal variation of the $\chi_m T$ product for salts **1**, **2** and **3**. (b) ESR spectra at room temperature of salts **1**, **2** and **3**.

weakly interacting within the perylene chain in an antiferromagnetic fashion. This result is in agreement with the considerable dilution of these electrons in the chain (one electron spin every four perylene molecules) and agrees with the picture of Fig. 4c where the unpaired electrons are in the half-filled band. In the three cases the above results support the charge distribution stated before, under the assumption that the C molecules are neutral.

The ESR spectra at room temperature of salts **1** and **2** are very similar (Fig. 5b). They present a very weak single narrow line at *g*-values of 2.0021 and 2.0026, respectively, with linewidths of 1.5 G in both salts. The weak intensity of the signals agrees with the fact that they come from paramagnetic impurities, probably perylene radicals as both *g*-values and linewidths are similar to those reported in other perylene radical salts.[8,16b] The ESR spectrum of salt **3** is somewhat different. It presents at room temperature a more intense and anisotropic line at $g = 2.0020$ with a linewidth of 3.0 G. Studies as a function of temperature are in progress.

Electrical transport measurements were performed on the best developed face of the single crystals in the temperature range 160–300 K for electrical conductivity and 120–300 K for thermopower. The plot of the logarithm of the electrical conductivity, log σ, *versus* the reciprocal temperature, $1000/T$, (Fig. 6a) clearly shows semiconducting behaviour with constant activation energy for the three salts. In salt **3** the room temperature conductivity (3 S cm^{-1}) is higher than in salts **1** and **2** (0.2 and 0.8 S cm^{-1}, respectively) and the activation energy (129 meV) is about half those of salts **1** and **2** (194 and 212 meV, respectively, see Table 2). This result reflects the

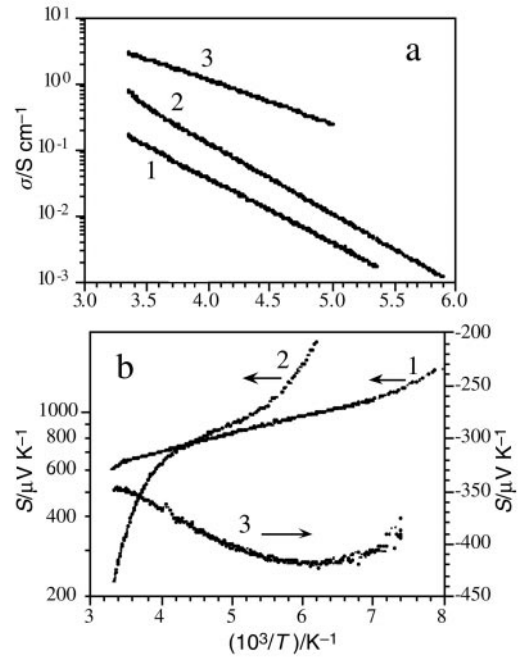

Fig. 6 Plots of the logarithm of the electrical conductivity (a) and of the Seebeck coefficient (b) *versus* $1000/T$ for salts **1**, **2** and **3**.

Table 2 Electrical transport and thermopower parameters for salts **1**, **2** and **3**

Salt	$\sigma_{300\ K}$/S cm^{-1}	E_a/meV	S/μS K^{-1}
(per)$_5$[Mo$_6$O$_{19}$] (**1**)	0.2	194	610
(per)$_5$[W$_6$O$_{19}$] (**2**)	0.8	212	230
(per)$_5$[VW$_5$O$_{19}$] (**3**)	3.0	129	−350

presence of an extra electron in the organic chains in salt **3** and the different band-filling mode.

Thermoelectric power, S, measurements (Fig. 6b) present large values (610, 230 and $-350\ \mu V\ K^{-1}$ for **1**, **2** and **3**, respectively, Table 2) that vary linearly with $1/T$, both confirming the semiconducting behaviour observed in the electrical conductivity. However, as seen in **2** and to a lesser extent in **3**, the slope of the S *vs.* $1/T$ plot is not constant over the whole temperature range, changing in the low temperature range. This is attributed to a change from intrinsic to extrinsic semiconducting behaviour. This change of regime is not seen in the electrical conductivity measurements as they could not be extended to such low temperatures.

Salts **1** and **2** present positive values of the Seebeck coefficient indicating hole dominated electrical conduction, while salt **3** presents negative values indicative of higher electron mobility. Again this change denotes the different band filling.

Conclusions

In this work we have reported the first examples of perylene based radical salts containing Lindquist-type polyoxometalate clusters as counterions. We have found that these large polyanions yield an unprecedented one-dimensional packing of the perylene donors where the chains display a criss-cross type arrangement formed by two alternating dimers. On the other hand, the possibility of varying the anionic charge while maintaining the structure of the polyoxometalate has enabled the control of the electronic band filling in the resulting salt, and therefore, the physical properties. Thus, the introduction of polyoxometalates with the same size and shape but different charges (−2 and −3) has resulted in marked changes in both transport and magnetic properties. For example, by adjusting the charge of the anion, the charge carriers responsible for conductivity were found to be either positive (for the dianions $[Mo_6O_{19}]^{2-}$ and $[W_6O_{19}]^{2-}$) or negative (for the trianion $[VW_5O_{19}]^{3-}$); at the same time, the magnetic properties changed from almost diamagnetic to paramagnetic. In the present work we used relatively small and weakly charged hexametallic non-magnetic anions. Novel semiconductors with high conductivities were obtained in this way. In the near future we plan to extend this kind of hybrid approach to other polyoxometalates having larger nuclearities, higher charges and/or more interesting electronic properties (*i.e.*, magnetic character and electron delocalization).

Experimental

Synthesis of the radical salts

The radical salts were obtained on a platinum wire electrode by anodic oxidation of the organic donor perylene (5 mg) in a U-shaped electrocrystallization cell in the presence of the tetrabutylammonium salt of the Lindquist polyanion (100 mg). The used solvents were dichloromethane for compound **1**, and a mixture of dichloromethane and acetonitrile (7 : 3 for compound **2** and 5 : 5 for compound **3**) with a total volume of 10 mL. Stable black needle-shaped (for **1** and **3**) and plate-like (for **2**) single crystals were obtained after one week with a current intensity of 0.6 μA. The tetrabutylammonium salts of the Lindquist polyoxoanions were obtained following the methods reported in the literature.[18] Perylene was purchased from Fluka.

X-Ray crystallographic analysis

Relevant details of data collection procedures and structure refinements for the crystallographic studies are given in Table 1. The atomic coordinates, thermal parameters, bond distances and bond angles of the asymmetric unit of the two salts are given in ESI.† Black shiny prismatic single crystals of suitable size of **1** and **3** (approximate dimensions: $0.40 \times 0.25 \times 0.20\ mm^3$ and $0.18 \times 0.17 \times 0.15\ mm^3$, respectively) were attached to a glass fibre and mounted on a goniometer head in a general position. Data for crystal **1** were collected on an Enraf-Nonius CAD4 diffractometer (graphite-monochromated MoK_α radiation) using the ω–2θ method. Cell parameters of **1** and **2** were obtained by the least-squares refinement of the setting angles of 25 reflections. The measurement of three standard reflections every 120 minutes revealed no intensity fluctuations. Absorption correction was applied by the method of North *et al.*[19] (semi-empirical ψ-scans). Data for crystal **3** were collected on a Siemens Smart CCD diffractometer (graphite-monochromated MoK_α radiation) and were corrected semiempirically for absorption and crystal decay (transmission 0.76–1.00). Both crystal structures were solved *ab initio* by direct methods using SIR97.[20] Refinement (SHELX97)[21] was by full-matrix least squares on F^2. All non-hydrogen atoms were allowed anisotropic thermal motion. Hydrogen atoms were assigned to ideal positions and refined using a riding model.

In the crystal structure of compound **3**, the refinement of the occupancy of the vanadium atom indicates that it is randomly distributed on the three independent metallic sites of the polyanion $[VW_5O_{19}]^{3-}$, which is located on an inversion centre.

CCDC reference numbers 161773–161774. See http://www.rsc.org/suppdata/jm/b1/b103032a/ for crystallographic data in CIF or other electronic format.

Conductivity and thermopower measurements

D.C. conductivity measurements over the range 150–300 K were performed with the standard four contacts method for all the samples along the long axis of several single crystals of each sample, giving reproducible results in all cases. Contacts to the crystals were made by platinum wires (20 μm diameter) attached by graphite paste to the samples. Thermoelectric power was measured along the long axis of the crystals by a slow a.c. ($\sim 10^{-2}$ Hz) technique, using an apparatus[22] similar to that described by Chaikin and Kwak[23] but computer controlled. The crystals were connected with platinum paint to gold wires (25 μm diameter) thermally anchored to two quartz blocks that were alternately heated. The thermal gradients across the sample were kept below 1 K and monitored by a Au (0.07 at.% Fe)–chromel thermocouple attached to the quartz reservoirs and measured with a Keithley 181 nanovoltmeter. A similar thermocouple attached to a quartz block was used to measure the sample temperature. The thermoelectric voltage was measured with a Keithley 181 nanovoltmeter and the absolute thermopower was calculated after correction for the absolute thermopower of the gold wires using the data of Huebner.[24]

Magnetic measurements

Variable temperature susceptibility measurements were carried out in the temperature range 2–300 K at a magnetic field of 1 T on polycrystalline samples with a magnetometer (Quantum Design MPMS-XL-5) equipped with a SQUID sensor. The susceptibility data were corrected from the sample holders previously measured under the same conditions and from the

diamagnetic contributions of the salts as deduced by using Pascal's constant tables. Room-temperature X-band ESR spectra were recorded on polycrystalline samples with a Bruker ELEXSYS E500 spectrometer. The field was measured using a diphenylpicrylhydrazyl (DPPH, $g = 2.0036$) stable free radical marker.

Acknowledgements

This work was developed in the framework of the COST Action D14 (Project on Inorganic Molecular Conductors). It was supported by the Spanish Ministerio de Ciencia y Tecnología (Grant MAT98-0880 and predoctoral fellowship to E. M.-F).

References

1 P. Day, M. Kurmoo, T. Mallah, I. R. Marsden, R. H. Friend, F. L. Pratt, W. Hayes, D. Chasseau, J. Gaultier, G. Bravic and L. Ducasse, *J. Am. Chem. Soc.*, 1992, **114**, 10722.
2 (*a*) M. Kurmoo, A. W. Graham, P. Day, S. J. Coles, M. B. Hurtshouse, J. L. Caulfield, J. Singleton, F. Pratt, W. Hayes, L. Ducasse and P. Guionneau, *J. Am. Chem. Soc.*, 1995, **117**, 12209; (*b*) H. Kobayashi, H. Tomita, T. Naito, A. Kobayashi, F. Sakai, T. Watanabe and P. Cassoux, *J. Am. Chem. Soc.*, 1996, **118**, 368.
3 E. Coronado, J. R. Galán-Mascarós, C. J. Gómez-García and V. N. Lauhkin, *Nature*, 2000, **408**, 447.
4 E. Coronado and C. J. Gómez-García, *Chem. Rev.*, 1998, **98**, 273 and references therein.
5 (*a*) S. Triki, L. Ouahab, D. Grandjean, R. Canet, C. Garrigou-Lagrange and P. Delhaes, *Synth. Met.*, 1993, **55–57**, 2028; (*b*) E. Coronado, J. R. Galán Mascarós, C. Gimenez-Saiz, C. J. Gómez-García and V. N. Lauhkin, *Adv. Mater.*, 1996, **8**, 801.
6 L. Ouahab, M. Bencharif, A. Mhanni, D. Pelloquin, J. F. Halet, O. Peña, J. Padiou, D. Grandjean, C. Garrigou-Lagrange, J. Amiell and P. Delhaes, *Chem. Mater.*, 1992, **4**, 666.
7 (*a*) C. J. Gómez-García, C. Giménez-Saiz, S. Triki, E. Coronado, P. L. Magueres, L. Ouahab, L. Ducasse, C. Sourisseau and P. Delhaes, *Inorg. Chem.*, 1995, **34**, 4139; (*b*) E. Coronado, J. R. Galán-Mascarós, C. Giménez-Saiz, C. J. Gómez-García and S. Triki, *J. Am. Chem. Soc.*, 1998, **120**, 4671.
8 M. Almeida and R. T. Henriques, in *Handbook of Organic Conductive Molecules and Polymers, vol. 1*, ed. H. S. Nalwa, John Wiley, Chichester, 1997, p. 87.
9 H. Akamatu, H. Inokuchi and Y. Matsunaga, *Bull. Chem. Soc. Jpn.*, 1956, **29**, 213.
10 H. C. I. Kao, M. Jones and M. M. Labes, *J. Chem. Soc., Chem. Commun.*, 1979, 329.
11 D. Schweiter, I. Henning, K. Bender, H. Endres and H. J. Keller, *Mol. Cryst. Liq. Cryst.*, 1985, **120**, 213.
12 (*a*) H. J. Keller, D. Nöthe, H. Pritzkov, D. Wehe, M. Werner, P. Koch and D. Schweitzer, *Mol. Cryst. Liq. Cryst.*, 1980, **62**, 181; (*b*) W. Brütting and W. Riess, *Acta Phys. Pol. A*, 1995, **87**, 785.
13 I. J. Tickle and C. K. Prout, *J. Chem. Soc., Perkin Trans. 2*, 1973, 720.
14 H. Hokado, K. Hasewaga and W. G. Schneider, *Can. J. Chem.*, 1964, **42**, 1084.
15 J. A. Ayllón, I. C. Santos, R. T. Henriques, M. Almeida, E. B. Lopes, J. Morgado, L. Alcácer, L. F. Veiros and M. T. Duarte, *J. Chem. Soc., Dalton Trans.*, 1995, 3543.
16 (*a*) V. Gama, M. Almeida, R. T. Henriques, I. C. Santos, A. Domingos, S. Ravy and J. P. Pouget, *J. Phys. Chem.*, 1991, **95**, 4263; (*b*) V. Gama, R. T. Henriques, G. Bonfait, L. C. Pereira, J. C. Waerenborgh, I. C. Santos, M. T. Duarte, J. M. P. Cabral and M. Almeida, *Inorg. Chem.*, 1992, **31**, 2598.
17 D. S. Rosseinsky and P. Kathirgamanathan, *J. Chem. Soc., Perkin Trans. 2*, 1985, 135.
18 (*a*) N. H. Hur, W. G. Klemperer and R. C. Wang, *Inorg. Synth.*, 1990, **27**, 77; (*b*) M. Fournier, *Inorg. Synth.*, 1990, **27**, 80; (*c*) C. M. Flynn Jr. and M. T. Pope, *Inorg. Chem.*, 1971, **10**, 2524.
19 A. C. T. North, D. C. Phillips and F. S. Mathews, *Acta Crystallogr., Sect. A*, 1968, **24**, 351.
20 SIR97, A. Altomare, M. C. Burla, M. Camalli, G. Cascarano, C. Giacovazzo, A. Guagliardi, A. G. G. Moliterni, G. Polidori and R. Spagna, *J. Appl. Crystallogr.*, 1999, **32**, 115.
21 G. M. Sheldrick, SHELX97: Programs for Crystal Structure Analysis, University of Göttingen, Germany, 1997.
22 M. Almeida, L. Alcácer and S. Oostra, *Phys. Rev. B*, 1984, **30**, 2839.
23 P. M. Chaikin and J. F. Kwak, *Rev. Sci. Instrum.*, 1975, **46**, 218.
24 R. P. Huebner, *Phys. Rev.*, 1964, **135**, A1281.